

Fabrication of large addition energy quantum dots in graphene

J. Moser^{1,*} and A. Bachtold^{1,†}

¹*CIN2 (CSIC-ICN) Barcelona, Campus UAB, E-08193 Bellaterra, Spain*

We present a simple technique to fabricate graphene quantum dots in a cryostat. It relies upon the controlled rupture of a suspended graphene sheet subjected to the application of a large electron current. This results in the *in-situ* formation of a clean and ultra-narrow constriction, which hosts one quantum dot, and occasionally a few quantum dots in series. Conductance spectroscopy indicates that individual quantum dots can possess an addition energy as large as 180 meV. Our technique has several assets: (i) the dot is suspended, thus the electrostatic influence of the substrate is reduced, and (ii) contamination is minimized, since the edges of the dot have only been exposed to the vacuum in the cryostat.

Graphene can be seen as a giant, flat molecule whose shape can be tailored by means of standard fabrication techniques. One long term goal is to structure graphene down to a small molecule, such as a benzene ring, connected to two graphene electrodes. A significant step in this direction has been achieved with the fabrication of chains of carbon atoms using the electron beam of an electron microscope to knock off the atoms of a graphene sheet [1]. Top-down fabrication strategies to structure graphene represent an original approach to realize devices in molecular electronics. Indeed, studying charge transport across molecules has so far been relying on a bottom-up approach, whereby the molecule under study is typically synthesized via chemical means and later on placed between two large metal electrodes. In this configuration, the contacted molecule often acts as a quantum dot, and the addition energy E_{add} needed to add one electron has been measured to be 100-400 meV [2, 3, 4, 5].

In this Letter, we present a technique to fabricate quantum dots out of a graphene sheet, under high vacuum and at low temperature in a cryostat. It is based on the controlled rupture of a suspended graphene sheet subjected to a large electron current, resulting in the formation of a quantum dot with an addition energy as large as 180 meV. Even though this energy is large, simple estimates show that the size of the quantum dot is of the order of 10 nm, that is the size of a large molecule.

We start with a description of our fabrication process. Our substrates are highly doped silicon wafers coated with 440 nm of thermal silicon oxide. We thoroughly clean the oxide surface in ozone in order to remove adsorbed hydrocarbon chains. Shortly afterwards, we deposit graphene sheets on the oxide surface using the scotch tape technique [6]. We identify single layer graphene sheets among thicker flakes by measuring the reflected light intensity using the blue channel of a CCD camera mounted on a Nikon optical microscope. We reduce the width of the middle region of the graphene sheet down to ~ 200 nm using electron beam lithography (EBL) followed by reactive ion etching in oxygen (see white contour in Fig. 1(b)). We pattern source and drain electrodes by EBL and Cr/Au thermal deposition.

At this point, we remove contamination by annealing the device at 300°C in flowing Ar/H₂ for a few hours. We then suspend the graphene sheet by removing the oxide in an aqueous solution of hydrofluoric acid (Fig. 1(a)). We expect that, by this stage of the process, only those oxide regions that are masked by graphene sheets have remained hydrocarbon-free (owing to the ozone treatment), and thus hydrophilic. As a result, the etching solution can rapidly diffuse between graphene and the oxide surface. This guarantees that even large graphene sheets are freely suspended. The oxide etched away, we critically dry the device. During this fabrication step, the sheet is always observed to fold on each side of the constriction (compare white contour before wet etching with the actual shape of the sheet in Fig. 1(b)).

At $T = 15$ K and under high vacuum ($< 10^{-6}$ mbar), we employ the current-induced cleaning technique [7] to remove adsorbates off the surface of the graphene sheet, which reduces extrinsic doping. A two-point measurement of the conductance as a function of the bias applied to the silicon substrate (backgate bias V_g) shows a conductance minimum close to zero V_g for some devices (top curve in Fig. 1(e)).

Passing a larger current between the source and drain electrodes drives the device to near mechanical rupture and forms an ultra-narrow constriction (see arrow in Figs. 1(c), 1(d)). Depending on the width of the patterned middle region, rupture is observed for currents ranging from 100 to 200 μA , consistent with the typical breakthrough current of graphene of about 1 $\mu\text{A}/\text{nm}$ [8]. The rupture occurs in the vicinity of the patterned middle region: the reduced cross-section ensures that the current density is largest, which favors the rupture. Upon reaching maximum current, the conductance exhibits large jumps [9, 10]. As soon as the conductance falls to a fraction of its low current value, a computer controlled feedback loop takes the current back to zero within ~ 10 msec. The lower conductance is consistent with the formation of a narrower constriction.

Following this large current treatment, we find that the low source-drain bias conductance G of the graphene sheet oscillates as a function of backgate bias V_g

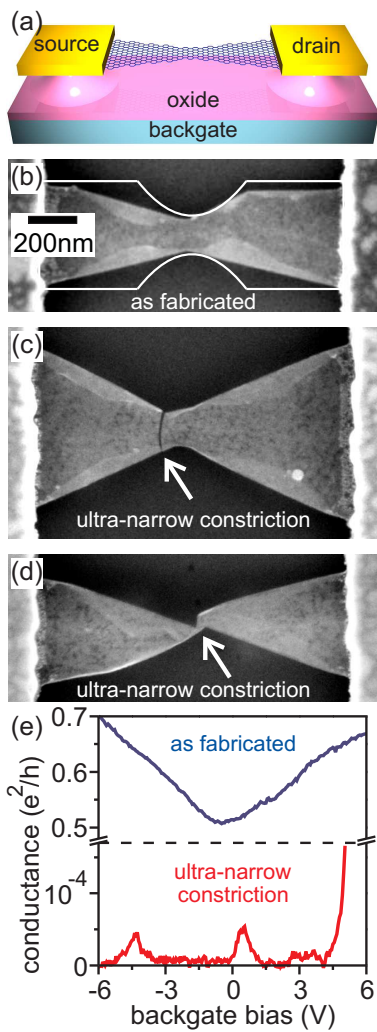


FIG. 1: (color) (a) Schematic of our device, showing a suspended graphene sheet contacted by source and drain electrodes. (b) Scanning electron microscope image of the device (top view) before rupture of the graphene sheet. The white contour indicates the shape of the sheet measured by atomic force microscopy prior to oxide removal. The edges of the sheet fold during fabrication of the suspended device. (c), (d) A large current induces a rupture of the sheet (arrow), shown here for two samples. In (d), the sheet is shown to break and then fold. (e) Two-point conductance vs. backgate bias at $T = 10$ K, before (blue trace) and after (red trace) breaking of the sheet. Note the two conductance scales. For this device, conductance oscillations are not periodic, and the stability diagram (not shown) suggests the presence of SET's in series.

(Fig. 1(e)). Measuring the differential conductance dI/dV as a function of source-drain bias V and V_g can yield well defined Coulomb diamonds for some devices, which indicate the presence of electron charging islands [11] in the ultra-narrow constriction. Figs. 2(a) and 2(b) display typical examples of such Coulomb diamonds, measured in two different samples at $T = 10$ K. In Fig. 2(a), the almost constant width of the diamonds

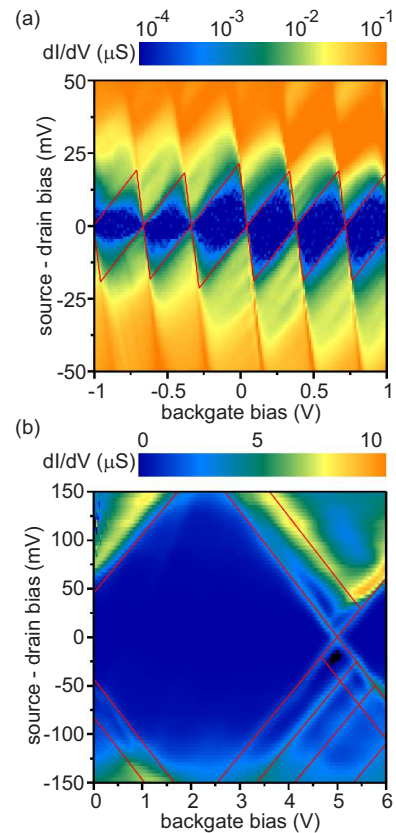


FIG. 2: (color) Differential conductance dI/dV as a function of source-drain bias V and backgate bias for two samples (a), (b) at $T = 10$ K. Red lines are guides to the eye.

(along the backgate bias axis), their constant slopes (highlighted by red lines), and the fact that diamonds are closed, all indicate the presence of one single electron island in the ultra-narrow constriction. In the Coulomb blockade regime, the diamonds height along the V -axis is a measure of the energy E_{add} to add one charge carrier to the island. In Fig. 2(a), $E_{\text{add}} \simeq 20$ meV. In Fig. 2(b), we measure a strikingly large E_{add} of ~ 180 meV. This value is nearly one order of magnitude larger than E_{add} in graphene single electron transistors nanofabricated so far [12, 13, 14, 15, 16]. Our fabrication technique has a reasonable yield: out of 7 devices studied, 3 exhibited single-electron transistor (SET) behavior over the range of backgate biases explored, 2 showed signatures of a series of SET's, 1 exhibited a particularly large $I(V)$ gap of ~ 700 mV at $T = 10$ K (which at present is not understood), and 1 failed during the high current treatment [17].

Fig. 2(b) shows additional conduction channels that appear at larger V as dI/dV resonances running parallel to the diamond edges. Fig. 3 shows dI/dV curves as a function of V_g at various values of V and at a bath temperature of 50 mK for the same sample. The energy spacing between consecutive conduction channels, given by V

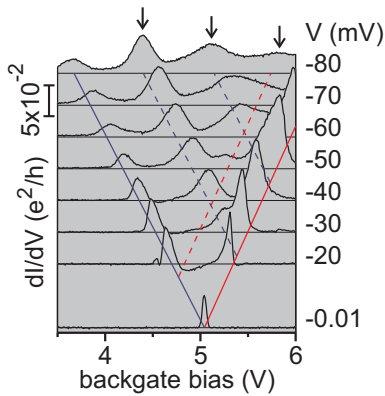


FIG. 3: (color) Differential conductance dI/dV traces, offset for clarity, as a function of backgate bias and at various source-drain biases V at $T = 50$ mK for the sample of Fig. 2(b). dI/dV resonances indicated by arrows are presumably related to excited states.

at the onset of a dI/dV resonance, is $\delta E \simeq 25$ meV [18]. These resonances are suggestive of transport mediated by excited states in the dot. Indeed, strong spatial confinement gives rise to a spectrum of zero-dimensional (0-D) levels that host excited states above the lowest available quantum level (ground state) [19, 20]. These 0-D excited states open up additional transport channels in the non-linear regime (larger V), and have been clearly observed in graphene quantum dots [13, 14].

We can obtain a rough estimate for the size d of our quantum dot in Fig. 2(b) using the measured addition energy E_{add} . Using the disk model, $d = e^2/(4\epsilon_0 E_C) \simeq 24$ nm, where ϵ_0 is the vacuum permittivity, and assuming that the charging energy $E_C \simeq E_{\text{add}}$. Another estimate can be obtained by comparing E_{add} to values measured by others for graphene dots of various sizes, assuming similar capacitive couplings. Ponomarenko and coworkers [12] studied several graphene quantum dots whose diameters range from 40 nm to 250 nm. When we plot their measured E_{add} as a function of dot diameter d , we find that E_{add} scales roughly as $E_{\text{add}} \simeq 500 \text{meV} \cdot \text{nm}/d$. Assuming that E_{add} is predominantly given by the charging energy E_C and taking into account that the average dielectric constant felt by the suspended graphene sheet in our configuration is about twice smaller, we estimate that the diameter of our quantum dot is ~ 6 nm. Overall, our dot size is on the ~ 10 nm scale. Finally, we estimate the number N of charge carriers in the graphene dot assuming a disk of diameter $d = 10$ nm and provided that $\delta E = 25$ meV, which reads $N = (\hbar v_F/d\delta E)^2 \simeq 10$ [13]. Surprisingly, this indicates a very large charge density of $\sim 10^{13}/\text{cm}^2$. Such a large density may originate from chemical doping by molecules [21] (still present under high vacuum) that have interacted with the dangling bonds at the edges of the dot.

We now comment on a possible mechanism driving the

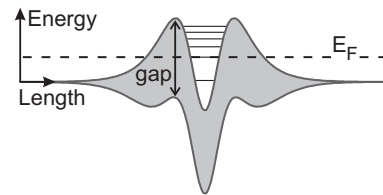


FIG. 4: Proposed potential landscape giving rise to 0-D confinement. The ultra-narrow constriction opens a gap at the Dirac point. On top of this gap, a fluctuating potential defines the quantum dot.

formation of our quantum dots. Due to its finite width, the ultra-narrow constriction created by the current-induced rupture of the graphene sheet may act as a hard wall confinement potential for charge carriers that opens an energy gap at the Dirac point, as observed in graphene nano-ribbons [16, 22]. Following Todd, *et al.* [15], and Stampfer, *et al.* [16], we propose that charge carriers become localized by potential fluctuations along the ultra-narrow constriction. These fluctuations may originate from the molecules [21] having reacted with the dangling bonds at the edges of the dot. Fig. 4 illustrates this scenario, where a fluctuating potential defines 0-D states above the energy gap created by the ultra-narrow constriction.

The mechanical robustness of our suspended devices is also noteworthy. Because graphene sheets, in every likelihood, contain finite build-in strain, it is remarkable that our tiny dots, which are only weakly connected to two sections of free standing graphene sheets, can exist at all. Presumably, the folding of the sheet along the edges make the graphene sheet stiffer (Fig. 1(b)), and the overall device mechanically more stable.

In conclusion, we have shown that the rupture of a graphene sheet subjected to a large current can be harnessed to fabricate graphene quantum dots endowed with a large addition energy. The fabrication minimizes the influence of the environment, since the dots are formed under high vacuum in a cryostat (keeping contamination to a minimum) and the dots are suspended (reducing electrostatic interaction with the substrate). In the future this technique might be improved to enable the control of the dot size (perhaps down to a single atom). For this, a conductance monitoring system operable on a much faster time scale is required. In addition, working in a cleaner gas environment may allow to better control the chemistry at the edges. For instance, the rupture of the sheet could be carried out in ultra-pure hydrogen in order to terminate carbon atoms with hydrogen atoms. Our suspended graphene quantum dots are potentially interesting nanoelectromechanical systems. Suspended graphene can act as a mechanical resonator whose vibrations could be coupled to charge transport through the quantum dot, as demonstrated in other materials [23].

We are grateful to A. Barreiro for help with fabrication and acknowledge fruitful discussions with J. Güttinger. This work was supported by an EURYI grant and FP6-IST- 021285-2.

* Electronic address: moser.joel@gmail.com

† Electronic address: adrian.bachtold@cin2.es

- [1] C. Jin, H. Lan, L. Peng, K. Suenaga, and S. Iijima, *Phys. Rev. Lett.* **102**, 205501 (2009).
- [2] S. Kubatkin, A. Danilov, M. Hjort, J. Cornil, J.-L. Brédas, N. Stuhr-Hansen, P. Hedegård, and T. Bjørnholm, *Nature* **425**, 698 (2003).
- [3] E. A. Osorio, K. O'Neill, N. Stuhr-Hansen, O. F. Nielsen, T. Bjørnholm, and H. S. J. van der Zant, *Advanced Materials* **19**, 281 (2007).
- [4] D. R. Ward, G. D. Scott, Z. K. Keane, N. J. Halas, and D. Natelson, *J. Phys: Condens. Matter* **20**, 374118 (2008).
- [5] N. Roch, S. Florens, V. Bouchiat, W. Wernsdorfer, and F. Balestro, *Nature* **453**, 633 (2008).
- [6] K. S. Novoselov, A. K. Geim, S. V. Morozov, D. Jiang, Y. Zhang, S. V. Dubonos, I. V. Grigorieva, A. A. Firsov, *Science* **306**, 666 (2004).
- [7] J. Moser, A. Barreiro, and A. Bachtold, *Appl. Phys. Lett.* **91**, 163513 (2007).
- [8] A. Barreiro, M. Lazzeri, J. Moser, F. Mauri, and A. Bachtold, *Phys. Rev. Lett.* **103**, 076601 (2009).
- [9] B. Standley, W. Bao, H. Zhang, J. Bruck, C. N. Lau, M. Bockrath, *Nano Letters* **8**, 3345 (2008).
- [10] Y. Li, A. Sinitskii, and J. M. Tour, *Nature Mater.* **7**, 966 (2008).
- [11] For a review, see J. Weis, *Single Electron Devices*, Lect. Notes Phys. **658**, 87 (2005).
- [12] L. A. Ponomarenko, F. Schedin, M. I. Katsnelson, R. Yang, E. W. Hill, K. S. Novoselov, and A. K. Geim, *Science* **320**, 356 (2008).
- [13] S. Schnez, F. Molitor, C. Stampfer, J. Güttinger, I. Shorubalko, T. Ihn, and K. Ensslin, *Appl. Phys. Lett.* **94**, 012107 (2009).
- [14] J. Güttinger, C. Stampfer, F. Libisch, T. Frey, J. Burgdörfer, T. Ihn, and K. Ensslin, *Phys. Rev. Lett.* **103**, 046810 (2009).
- [15] K. Todd, H.-T. Chou, S. Amasha, and D. Goldhaber-Gordon, *Nano Lett.* **9**, 416 (2009).
- [16] C. Stampfer, J. Güttinger, S. Hellmüller, F. Molitor, K. Ensslin, and T. Ihn, *Phys. Rev. Lett.* **102**, 056403 (2009).
- [17] The stability diagrams of some of our devices revealed a series of dots, yet they were not significantly altered by subsequent high current treatments.
- [18] The analysis of the thermal linewidth of conductance resonances at low V leads to the lever arm conversion between V_g and the actual change in the electrochemical potential, which is consistent with the slope of the diamond in Fig. 2(b).
- [19] A. T. Johnson, L. P. Kouwenhoven, W. de Jong, N. C. van der Vaart, and C. J. P. M. Harmans, and C. T. Foxon, *Phys. Rev. Lett.* **69**, 1592 (1992).
- [20] J. Weis, R. J. Haug, K. v. Klitzing, and K. Ploog, *Phys. Rev. Lett.* **71**, 4019 (1993).
- [21] J. Moser, A. Verdaguer, D. Jiménez, A. Barreiro, and A. Bachtold, *Appl. Phys. Lett.* **92**, 123507 (2008).
- [22] M. Y. Han, B. Oezylmaz, Y. Zhang, and P. Kim, *Phys. Rev. Lett.* **98**, 206805 (2007).
- [23] E.M.Weig, R. H. Blick, T. Brandes, J. Kirschbaum, W.Wegscheider, M. Bichler, and J. P. Kotthaus, *Phys. Rev. Lett.* **92**, 046804 (2004). R. Leturcq, C. Stampfer, K. Inderbitzin, L. Durrer, C. Hierold, E. Mariani, M. G. Schultz, F. von Oppen, and K. Ensslin, *Nat. Phys.* **5**, 327(2009). G. A. Steele, A. K. Hüttel, B. Witkamp, M. Poot, H. B. Meerwaldt, L. P. Kouwenhoven, and H. S. J. van der Zant, *Science* **325**, 1103 (2009). B. Lassagne, Y. Tarakanov, J. Kinaret, D. Garcia-Sanchez, and A. Bachtold, *Science* **325**, 1107 (2009).